ACS Catalysis

Research Article

pubs.acs.org/acscatalysis

Aminopolymer–Silica Composite-Supported Pd Catalysts for Selective Hydrogenation of Alkynes

Wei Long,[†] Nicholas A. Brunelli,[‡] Stephanie A. Didas,[‡] Eric W. Ping,[‡] and Christopher W. Jones*[,†,‡]

[†]School of Chemistry & Biochemistry and [‡]School of Chemical &Biomolecular Engineering, Georgia Institute of Technology, 311 Ferst Drive, Atlanta, Georgia 30332, United States

Supporting Information

ABSTRACT: A single-component, recyclable heterogeneous palladium nanoparticle catalyst is described for the selective hydrogenation of alkynes. The palladium nanoparticles are generated through reduction of Pd(II) species loaded into a mesoporous silica material functionalized with branched poly(ethyleneimine) polymers. An array of composite catalysts with similar polymer composition, palladium loading, and nanoparticle size (~2 nm) are prepared to understand the importance of the polymer attachment method, the metal reduction method, the polymer molecular weight, and the oxide porosity. Each catalyst shows excellent activity in room temperature, liquid phase hydrogenation of diphenylacetylene to selectively produce *cis*-stilbene. Interestingly, it was found that the rate of over-hydrogenation could be significantly reduced by increasing the support porosity and using a high-molecular-weight polymer. These single-component catalysts are competitive with the best palladium catalysts known for the selective liquid phase hydrogenation of alkynes and can be easily recovered and recycled with no leaching of palladium detected, retaining high activities and selectivities over multiple cycles with a simple regeneration procedure.

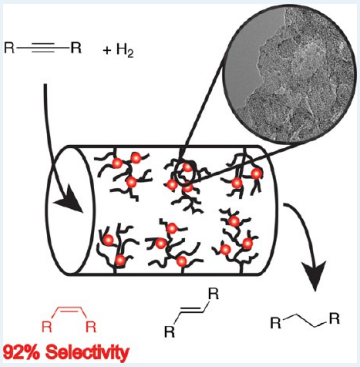

KEYWORDS: *palladium, nanoparticle, hyperbranched aminosilica, overhydrogenation, semihydrogenation*

1. INTRODUCTION

The selective hydrogenation of carbon–carbon triple bonds to double bonds is a catalytic challenge relevant to commodity chemical production (e.g., purification of olefin feeds for polymerization reactions) as well as for synthesis of fine and specialty chemicals.[1,2] Although a wide variety of catalysts have been developed for the selective hydrogenation of alkynes,[3−5] the key challenge remains preventing over-hydrogenation while achieving acceptable reaction rates.[6]

The Lindlar catalyst[7] (Pd on $CaCO_3$ poisoned with lead) is the prototypical example of a highly selective supported metal catalyst for liquid phase hydrogenation of alkynes created by addition of an appropriate surface modifier. For this catalyst, the lead is used as an irreversible dopant to promote the selective reduction of alkynes to *cis*-alkenes while a basic compound such as quinoline is often added during the reaction to slow the subsequent hydrogenation of the desired *cis*-alkene product to alkanes, thereby achieving a very high selectivity to *cis*-alkenes, even at a high alkyne conversion.[1] The outstanding selectivity is thus associated with the use of undesirable, toxic lead compounds and other soluble additives. Therefore, it is desirable to develop alternative, greener catalysts for this catalytic transformation.

The design of a better catalyst can be facilitated by understanding the underlying mechanisms that lead to the selective hydrogenation of alkynes to alkenes over palladium catalysts, but those are not yet fully understood (and may differ in gas phase vs liquid phase reactions). Nonetheless, much progress has been made recently, including identifying the important roles of surface and subsurface carbon,[8−12] the amount and nature of the palladium hydride species present during reaction,[13−15] and the role of surface modifiers such as CO or additional metal dopants.[16−19] Selectivity can either be achieved due to thermodynamic or kinetic effects. Thermodynamic effects involve altering the relative binding efficiency of the alkyne over the alkene (K_1 vs K_2), whereas kinetic effects involve modifying the relative rates of hydrogenation (k_1 and k_2). The traditional interpretation when using metallic palladium indicates that kinetic effects are less important than thermodynamic effects because the rates of hydrogenation of alkynes and alkenes are normally of the same order of magnitude. Selectivity is essentially governed by thermodynamic effects, more specifically, the adsorption strength of different unsaturated C–C bonds on the metal active sites.[1] Selectivity may be greatly enhanced by introducing surface modifiers that adsorb stronger than alkenes and weaker than alkynes to the surface (Scheme 1).[20] Modifiers can be added during the catalytic reactions: for example, N or S containing compounds for liquid phase hydrogenation of alkynes[21] or CO as a feed additive in the gas phase hydrogenation.[22] Dopants can also be incorporated into the original catalysts,[23,24] for example, by addition of a second metal,[25−29] or through the use of surfactants or polymers to adjust the selectivity of the catalysts.[30−35] Although the former approach provides better

Received: November 15, 2012
Revised: June 15, 2013
Published: June 21, 2013

   dx.doi.org/10.1021/cs3007395 | ACS Catal. 2013, 3, 1700−1708

Scheme 1. Reaction Routes of Selective Hydrogenation of Disubstituted Alkynes

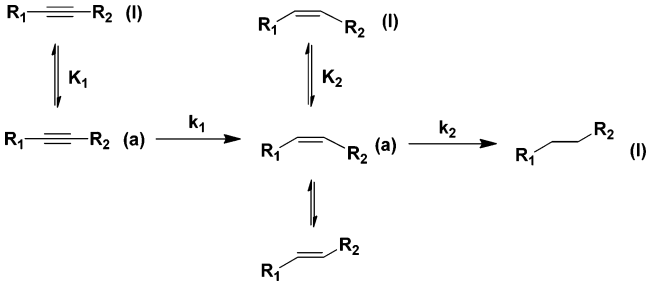

operational flexibility, the latter one facilitates recovery of the potentially expensive modifying agents or ligands, as well as simplifies the product purification process.

Many alternative palladium catalysts have been evaluated for alkyne semihydrogenation, including various supported Pd nanoparticles[36−44] and molecular Pd complexes.[45−52] For the nanoparticle catalysts, several approaches have been used to create catalysts that can selectively produce olefins from alkynes, such as manipulating metal nanoparticle dispersion or shapes[3,4] or applying various surface modifiers.[5] Naked, unsupported metal nanoparticles tend to aggregate due to their high surface energy, resulting in a decrease of catalytic activity over time due to nanoparticle sintering. To limit sintering, polymers or surfactants have been used for preparation of dispersed metal nanoparticles with good stability, with dendrimer-/polymer-encapsulated noble metal nanoparticles,[20,53,54] and surfactant-stabilized Pd colloids[55] as two examples. Although polymer-stabilized metal nanoparticles show unique catalytic properties in many cases, the inherent difficulties in separation of these soluble catalysts limits their wide application. For many applications, the surfactant or polymer capping agents must be removed to liberate the nanoparticle active sites and allow for good catalytic activity.[56]

Thus, much effort has been directed toward development of new catalytic systems with good activity and selectivity that are easy to separate and recycle,[39−43] such as mesoporous silica-supported Pd nanoparticles,[37,38,44] and Pd nanoclusters inside cross-linked polymer frameworks.[57] Polymer composites have also emerged as promising supports for metal nanoparticle catalysts[58,59] because of the possibility of tuning catalytic properties using the polymeric functional groups, easy recovery compared with soluble polymer/dendrimer encapsulated catalysts, and the ability to exert nanoscale control on metal cluster properties.

In this work, aminopolymer−silica composites are used to play two roles: first, to modify the reactivity of the incorporated Pd nanoclusters through the ligating amine sites, and second, to promote good dispersion of the nanoparticles. Mesoporous-silica-supported aminopolymer composites are prepared with both "grafting-to" and "grafting-from" methods. After immobilization of a Pd(II) precursor onto the polymer composite, two reduction methods (H_2 reduction and $NaBH_4$ reduction) were investigated to generate palladium nanoparticles within the polymer composite matrix. The resulting catalysts were evaluated in the selective hydrogenation of diphenylacetylene. The catalytic activity, selectivity, and recyclability were evaluated in detail to better understand the modification and stabilization effects of the aminopolymers. In contrast to cases in which the organic base modifier requires removal,[56] in this work, the aminopolymer modifier plays a crucial role in tuning the selectivity of the catalyst.

2. EXPERIMENTAL SECTION

2.1. Chemicals and Materials. The following chemicals were commercially available and used as received unless otherwise noted: Pluronic P123 EO−PO−EO triblock copolymer (poly(ethylene glycol)−poly(propylene glycol)−poly(ethylene glycol); $M_n \sim 5800$, Sigma-Aldrich), tetraethylorthosilicate (TEOS, 98%, Sigma-Aldrich), hydrochloric acid (HCl, 37%, EMD), 3-chloropropyltrimethoxysilane (Gelest), poly(ethylenimine) (branched, Sigma-Aldrich, M_n = 10 000, M_w = 25 000), palladium(II) acetate (98%, Sigma-Aldrich), sodium borohydride ($NaBH_4$, 99%, Sigma-Aldrich), ethanol (reagent grade, BDH), aqueous ammonia solution (28%, BDH), toluene (anhydrous, J.T. Baker), methanol (anhydrous, J.T. Baker), 1,4-dioxane (anhydrous, Alfa Aesar), diethylene glycol dibutyl ether (99+%, Acros), diphenylacetylene (98%, Sigma-Aldrich), ethyl phenylpropiolate (98%, Sigma-Aldrich), 2,5-dimethyl-3-hexyne-2,5-diol (98%, Acros), propargyl benzoate (98%, Sigma-Aldrich).

2.2. Characterization. A Netzsch STA 409 was used for thermal gravimetric analysis (TGA) of materials under a mixture of air and nitrogen with a heating rate of 10 °C min^{-1} from room temperature to 900 °C. Surface area, pore volume, and pore size distribution were assessed via nitrogen physisorption analysis using a Micromeritics Tristar II. Surface area was determined by the Brunauer−Emmett−Teller (BET) method. Pore volume and pore size were calculated via the Broekhoff−de Boer method with the Frenkel−Halsey−Hill modification (BdB−FHH).[60] FT-IR spectra were obtained on a Bruker Vertex 80 optical bench using KBr Pellets. X-ray photoelectron spectroscopy (XPS) was performed on a Thermo K-Alpha XPS using Al Kα irradiation with a flood gun. A thin layer of powder was dispersed on the surface of carbon tape, evacuated in a load lock, and then transferred into the analysis chamber (vacuum around 10^{-8} mbar) for measurement. The binding energy of different elements was corrected according to the Si 2p peak at 103.6 eV. Transmission electron microscopy (TEM) measurements were performed on Tecnai F30 with an accelerating voltage of 300 kV. Ultraviolet−visible spectroscopy (UV/vis) was performed on Agilent 8510 spectrophotometer for solution samples. Diffuse-reflectance UV/vis on solid samples was measured with an Ocean Optics USB 2000 fiber optic spectrometer using a PTFE sample as a diffuse reflectance standard. The reaction conversions were monitored by gas chromatography (GC) on a Shimadzu GC-2010 with a FID detector and a SHRX5 column. Elemental analyses were measured by Columbia Analytical Services (Tucson, AZ) and Atlantic Microlab (Atlanta, GA).

2.3. Preparation of Aminopolymer−Silica Composites. *SBA-15 Synthesis.* The mesoporous silica SBA-15 was synthesized according to published procedures,[61,62] and the reagents were scaled accordingly. The polymer template (Pluronic P123, 24 g) was dispersed in HCl (120 mL) and distilled H_2O (636 mL). After the polymer was dissolved completely, TEOS (46.26 g) was added, and the solution was stirred for 20 h at 40 °C. The solution was heated to 100 °C and maintained at this temperature for 24 h without stirring. At the end of synthesis, the mixture was quenched with distilled H_2O, filtered, and washed repeatedly with distilled H_2O. The recovered solid was dried in the oven at 75 °C overnight and

dx.doi.org/10.1021/cs3007395 | ACS Catal. 2013, 3, 1700−1708

then calcined in the oven according to the following temperature profile: (1) heating to 200 °C at 1.2 °C min^{-1}; (2) holding at 200 °C for 1 h; (3) heating to 550 °C at 1.2 °C min^{-1}; (4) holding at 550 °C for 6 h.

MCF Synthesis. Siliceous mesocellular foam (MCF) was synthesized according to a reported procedure with slight modifications.[63] The polymer template (Pluronic P123, 16.0 g) was dissolved in a mixture of HCl (47.4 g) and distilled H_2O (260 g). The solution was heated to 40 °C, and then 1,3,5-trimethyl benzene (16 g) was added. After 2 h of mixing, TEOS (34.6 g) was added. The mixture was stirred for 5 min and then maintained quiescently at 40 °C for 20 h. NH_4F (184 mg) in 20 mL of distilled H_2O was added as the mineralization agent, and the solution was swirled briefly before aging at 100 °C for 24 h. The resulting solid was recovered by filtration, washed repeatedly with distilled H_2O, dried, and calcined according to the following temperature profile: (1) heating to 550 °C at 1.0 °C min^{-1}; (2) holding at 550 °C for 6 h.

Preparation of HAS. Aziridine was synthesized and purified according to reported methods.[64,65] (Caution: Aziridine is a carcinogenic hazard. Please only handle it in a ventilated fume hood and wear proper personal protective equipment.) Hyperbranched amino silica (HAS) was synthesized following published procedures.[65] SBA-15 (1.0 g, dried under vacuum at 150 °C overnight before use) was dispersed into 50 mL of toluene, and the mixture was stirred for 1 h. Aziridine (2.0 g) was added into the solution under stirring, and acetic acid (4 drops) was added to catalyze the polymerization. The solution was stirred at room temperature for 24 h in a capped pressure vessel. The resulting material was recovered, washed repeatedly with toluene and methanol, and dried under vacuum around 65 °C overnight.

Preparation of SiO_2-gt-PEI. An aminopolymer silica composite was also prepared with a grafting-to method following published procedures with some modifications.[66] Silica (2.0 g, dried under vacuum at 150 °C overnight before use) was first dispersed into dry toluene (100 mL). Chloropropyltrimethoxysilane (3.7 g) was added into the slurry slowly, and the mixture was heated to 150 °C for 24 h. The solid was recovered by filtration through filter paper and washed with copious amounts of toluene, petroleum ether, methanol, and diethyl ether. Finally, the white powder was dried under vacuum at 100 °C overnight.

PEI (6.0 g) was dissolved completely in distilled H_2O (6.0 g) and ethanol (100 mL), and then the solution was degassed with argon for 30 min. The silica-supported propyl chloride material was added into the solution under argon, and stirring was continued at room temperature for 30 min. The mixture was stirred at 90 °C for 24 h. The resulting material was recovered, washed with distilled H_2O, ammonia solution (28 wt %), and methanol before drying under vacuum around 65 °C overnight.

2.4. Preparation of Supported Palladium Catalysts. In a typical procedure, the aminopolymer silica composite (1.0 g) was dispersed into anhydrous methanol (47 mL) under argon with stirring for 1 h, then $Pd(OAc)_2$ (23.5 mg) was transferred into the solution under argon, and the mixture was stirred at room temperature for 24 h. The resulting slightly yellow powder was recovered by filtration, washed three times with methanol, and dried under vacuum at room temperature. The resulting material was later reduced via two methods, (i) the H_2 reduction method or (ii) the $NaBH_4$ reduction method.

H_2 Reduction. Pd(II)−HAS (500 mg) was dispersed in anhydrous methanol (24 mL) under inert gas with stirring for about 1 h. Hydrogen was introduced to the reaction system via a needle to the solution. The hydrogen pressure was 0.1 MPa, and the flow rate was kept constant. The mixture was stirred under hydrogen for 64 h. At end of the reaction, methanol was removed under vacuum via a Schlenk line. The resulting powder was transferred into a glovebox, washed with anhydrous methanol, and filtered inside the glovebox. The recovered catalyst was dried under vacuum at room temperature and stored inside the glovebox for further use.

$NaBH_4$ Reduction. Distilled H_2O (75 mL) was degassed with argon for about 3 h before use. Pd(II)−HAS (800 mg) was dispersed into distilled H_2O (65 mL) with stirring for 30 min. After adding a freshly prepared $NaBH_4$ solution (284 mg $NaBH_4$ in 10 mL distilled H_2O), the color of the mixture rapidly darkened. The solution was stirred for additional 2 h, and the solids were recovered via filtration. The resulting catalyst was washed repeatedly with distilled H_2O and methanol, dried under vacuum, and stored under ambient conditions for further use. Other aminopolymer silica-supported Pd catalysts were prepared following similar procedures.

2.5. Selective Hydrogenation of Alkynes. Catalytic reactions were performed in a three-neck flask at room temperature and 0.1 MPa H_2. Hydrogen at a constant flow rate was introduced into the reactor through one side arm of the flask, and another side arm was connected to a condenser with −15 °C coolant circulating through it to limit evaporation of solvents. In a typical reaction with Pd−HAS (prepared by H_2 reduction), a small amount of catalyst (22 mg, 0.4 mol % Pd relative to the reactant) was transferred into the reactor inside a glovebox. Before reaction, the flask with the catalyst was purged with argon for about 20 min and then with H_2 for about 10 min. Substrate (0.5 mmol) was dissolved into anhydrous methanol (0.5 mL) and anhydrous 1,4-dioxane (0.5 mL) with diethylene glycol dibutyl ether (50 μL) as the internal standard. The reactant solution was degassed first with inert gas and then transferred into the reactor via a syringe to start the reaction. A small aliquot of sample was withdrawn at specific times, passed through a short silica column, diluted, and analyzed via GC−FID to monitor the course of the reaction.

For the catalysts prepared with $NaBH_4$ reduction, a much higher reaction rate was observed. To get reliable kinetic data, the catalyst amount was reduced to extend the reaction time for enough sampling points. Similarly, a small amount of catalyst (0.1 mol % Pd loading) was transferred into the flask, and the system was purged with argon for about 20 min and then with H_2 for about 10 min. Next, 1.5 mL of anhydrous methanol was added to disperse the catalyst, and then the solution was treated under H_2 for 24.5 h (room temperature, 0.1 MPa H_2 pressure). Reactant (1.5 mmol) was dissolved into anhydrous 1,4-dioxane (1.5 mL) with diethylene glycol dibutyl ether (150 μL) under inert gas, and then the solution was transferred into the flask to start the reaction. At the end of reaction, the catalysts were recovered by filtration, washed with copious amount of methanol, and then dried under vacuum at room temperature. The recovered powder was reused or kept for other characterization.

The internal and external mass transfer influences were assessed for a representative catalyst, Pd/SBA-gt-PEI. The details are provided in the Supporting Information. Under the conditions used here, the reaction is suggested to occur under a kinetic regime.

dx.doi.org/10.1021/cs3007395 | ACS Catal. 2013, 3, 1700−1708

2.6. Catalyst Regeneration. A small amount of recovered catalyst (Pd/SBA-gt-PEI-r, 45 mg) was transferred into a flask, and the system was purged with argon for 10 min. A freshly prepared $NaBH_4$ solution (0.1 M, 4.2 mL) was transferred into the flask quickly, and the solution was stirred for 1 h. The material was recovered, washed with distilled H_2O and methanol, and dried under vacuum at room temperature.

3. RESULTS AND DISCUSSION

3.1. Preparation and Characterization of Aminopolymer−Silica Composites. Mesoporous silica SBA-15 and MCF were successfully synthesized for use as supports for preparation of the aminopolymer−silica composites. After the in situ polymerization with aziridine, the polymer content of the aminopolymer−silica composites was estimated by TGA (Supporting Information Table S1). The HAS support had 22 wt % of polymer loading. For comparative analysis, SiO_2-gt-PEI materials with similar polymer contents were prepared via the grafting-to method (Scheme 2). According to elemental analysis, only a very small amount of Cl remained in the resulting materials, indicating the majority of the propyl chloride functional groups were reacted with PEI in the second step, and every polymer chain was anchored to multiple sites on the silica surface. In FT-IR spectra of the materials (Supporting Information Figure S1), the peaks at 2930 cm^{-1} were assigned to aliphatic C−H stretches, and the peak at 1483 cm^{-1} was assigned to C−H vibrations. The N−H vibration was clearly visible at 1580 and 1645 cm^{-1}, which further confirmed the successful incorporation of the aminopolymer into the materials.[67] A decrease in the surface area, pore size, and pore volume with increasing organic loading was observed in the nitrogen adsorption analysis (Supporting Information Table S2), confirming that the aminopolymer was infiltrated into the pores of the mesoporous silica.

Scheme 2. Preparation of Aminopolymer−Silica Composites HAS and SiO_2-gt-PEI

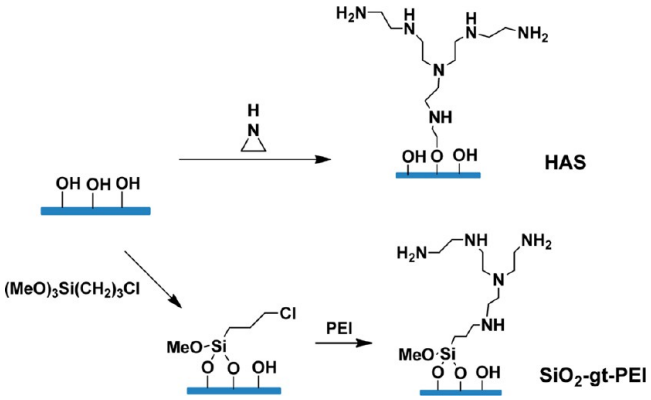

3.2. Preparation and Catalytic Performance of Pd−HAS. The HAS solid was metalated with palladium acetate in methanol for 24 h to introduce Pd(II) ions to the nitrogen ligands, and then the recovered material was washed with copious amounts of methanol to remove free or weakly bonded Pd(II) ions (Scheme 3). Pd(II)−HAS was further reduced with (a) hydrogen in methanol (room temperature, 0.1 MPa), following a method similar to that reported for reducing Pd(II)/PEI in the literature or (b) using $NaBH_4$, a strong reducing agent commonly used for producing metal nanoparticles, to yield the resulting catalyst Pd−HAS.

Although under similar conditions, homogeneous Pd(II)/PEI was readily reduced to Pd(0)−PEI (Figure S2),[30,32] the majority of the Pd species in Pd−HAS (H_2 reduction) still existed as Pd(II) species (see the Supporting Information). Catalysis with these precatalysts (not shown) gave a substantial induction period because additional time was needed to further reduce the palladium species to form nanoparticles. Therefore, $NaBH_4$ reduction was used as an alternative method for preparation of HAS-supported Pd nanoparticles. In UV−vis measurements, the decreased intensity of the peak at 300 nm (Pd(II) ligated to amine(s)), the appearance of a broad absorbance from 300 to 800 nm which decays gradually with increasing wavelength (Supporting Information Figure S3), and the gray color of the recovered catalysts all indicated the formation of palladium nanoparticles.[68,69] The material was further characterized with TEM and XPS (SI). In the TEM images (Figure 1A), nanoparticles ∼2 nm in diameter with a narrow particle distribution were clearly observed in the polymer composite, and XPS measurements revealed a considerable amount of Pd(0) formation.

The Pd−HAS catalyst prepared with $NaBH_4$ reduction displayed similar selectivity (Table 1) but substantially higher activity than the Pd−HAS (H_2 reduction) catalyst. The stronger reducing agent was necessary in this system to nucleate small particles. This observation also suggests that the activity in these catalysts is largely associated with Pd(0) nanoparticles, rather than molecular Pd(II) species ligated to the aminopolymer.

The catalytic performance of Pd−HAS ($NaBH_4$) was compared with other supported Pd catalysts tested under similar conditions (Table 1), including (a) the Lindlar catalyst with or without quinoline as a benchmark and (b) Pd/PEI as a silica-free analogue based on the soluble polymer (Table 1). The Lindlar catalyst and the Pd/PEI are highly selective catalysts, but the activities are significantly lower than Pd−HAS ($NaBH_4$) on a palladium basis. The aminosilica composite catalyst uniquely combines high activity and good selectivity, a combination not found simultaneously in the other catalysts.

Scheme 3. Preparation of Aminopolymer−Silica-Supported Pd Catalysts

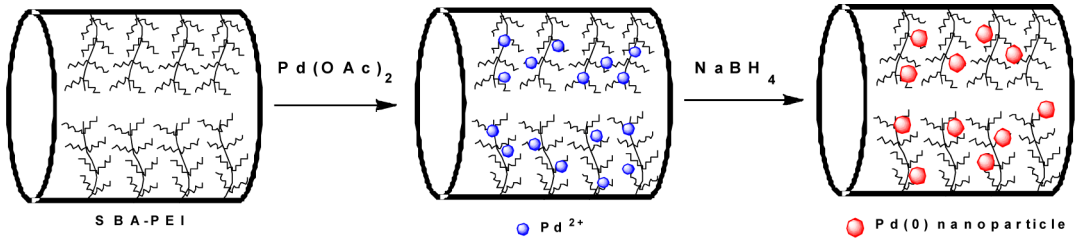

dx.doi.org/10.1021/cs3007395 | ACS Catal. 2013, 3, 1700−1708

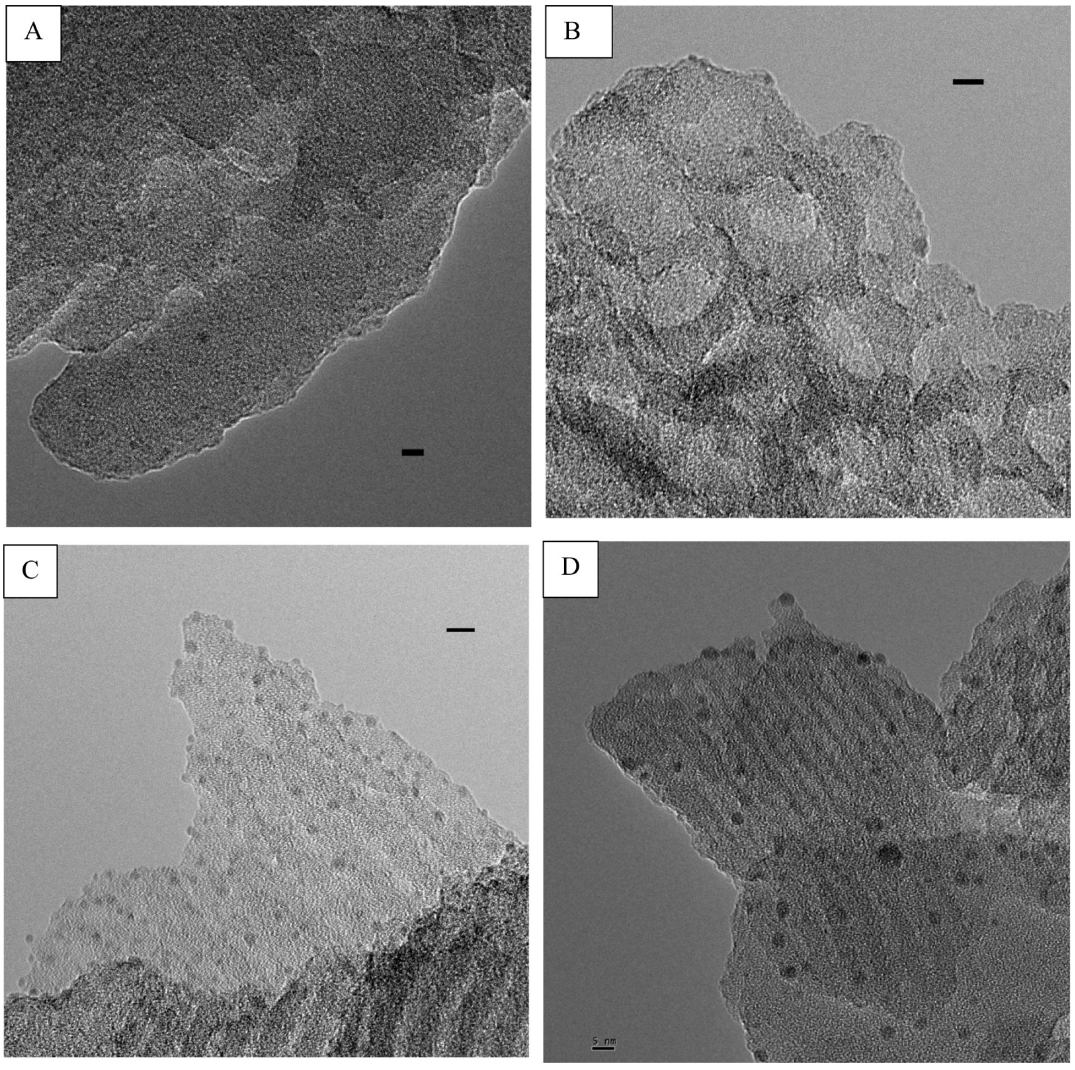

Figure 1. TEM of (A) Pd−HAS ($NaBH_4$ reduction), (B) Pd/MCF-gt-PEI, (C) Pd/SBA-gt-PEI, (D) Pd/SBA-gt-PEI (used). Scale bar: 5 nm.

Table 1. Catalytic Performance of Aminopolymer−Silica-Supported Pd Catalysts and Comparison with Other Supported Pd Catalysts

catalysts	time (h)	conv (%)	R^a(mol yne/mol Pd × hr)	selectivity[b]
Pd−HAS (H_2 reduction)	6	98	40	88:2:10
Pd−HAS ($NaBH_4$ reduction)	0.34	93	2389	91:4:5
Pd/SBA-gt-PEI	0.45	98	2170	90:4:6
Pd/MCF-gt-PEI	0.42	>99	2387	91:4:5
Lindlar[c]	3	99	333	95:2:3
Lindlar + quinoline[d]	7.5	99	133	96:2:2
Pd/PEI[e]	12	>99	10	95:1:4

[a]R = average rate of moles of alkyne consumed/(mol of Pd * time), the total amount of Pd was used and dispersion of nanoparticle was not taken into consideration for the calculation. For a discussion of estimated rates on Pd site basis, see the Supporting Information. [b]Determined by GC−FID after calibration. Selectivity = *cis*-alkene/*trans*-alkene/alkane. [c]This work. Reaction performed with 0.1 mol % Pd. [d]This work. Reaction performed with 0.1 mol % Pd and 1 mol % quinoline. [e]Reaction performed in MeOH:dioxane =1:1, room temperature, under an H_2 balloon, products determined by ^1H NMR.[30,32]

3.3. Catalytic Performance of Pd/SiO_2-gt-PEI. For HAS materials prepared via in situ polymerization of aziridine, the molecular weight of the resulting aminopolymer is normally several thousand Daltons.[70,71] Larger polymer molecular weights have thus far not been reported for HAS materials.[71] To allow for better control of the polymer structure within the composite support, we also investigated supported materials via the "grafting to" approach. Specifically, presynthesized PEI with a known structure and molecular weight was used (branched, as in HAS materials, $M_w \sim 25\,000$, $M_n \sim 10\,000$, d = 4.6 nm by DLS) as the polymer component, taking into account two considerations: (1) the polymer size should fit into the pores of mesoporous silica used in this work (SBA-15 and MCF) and (2) the polymer should provide protection and encapsulation of the Pd nanoparticle without preventing access to the substrates. Given these constraints, the above polymer was chosen. Two types of mesoporous silica, SBA-15 and MCF, were used for preparation of SiO_2-gt-PEI. SBA-15 is a highly ordered mesoporous silica composed of one-dimensional cylindrical channels and is the same support used to create the HAS materials. MCF consists of large, hollow, spherical cells and three-dimensional interconnecting cylindrical windows, providing enhanced pore connectivity and pore volume for loading of polymer-encapsulated Pd(0) nanoparticles.

dx.doi.org/10.1021/cs3007395 | *ACS Catal.* 2013, 3, 1700−1708

The Pd(0) nanoparticles in Pd/SBA-gt-PEI and Pd/MCF-gt-PEI were synthesized in the same manner as the Pd−HAS ($NaBH_4$ reduction) material. The composition of the catalyst was determined by elemental analysis, measuring the weight percent of Pd, C, H, N, and Si for each sample. For a fair comparison, the catalysts were prepared with similar palladium contents and Pd/N ratios (Table 2). Palladium nanoparticles

Table 2. Composition of the Aminopolymer−Silica Composite Catalysts, As Determined by Elemental Analysis

catalysts	Pd (wt %)	C (wt %)	N (wt %)	Pd/N
Pd−HAS ($NaBH_4$ reduction)	0.7	9.8	5.3	0.017
Pd/SBA-gt-PEI	1.1	14.7	6.6	0.022
Pd/MCF-gt-PEI	0.94	17.2	7.9	0.016

1.6 nm (Supporting Information Figure S4) in diameter with good dispersion in the 1D channels of SBA-15 were clearly observed in the HRTEM images of Pd/SBA-gt-PEI (Figure 1C). Similarly, the TEM images of Pd/MCF-gt-PEI showed well-dispersed Pd nanoparticles inside the large cells of the porous material (Figure 1B). The catalysts were also characterized with XPS to assess the oxidation state of the palladium, finding that the $NaBH_4$ reduction method produced a significantly amount of Pd(0).

The Pd−HAS ($NaBH_4$ reduction), Pd/SBA-gt-PEI, and Pd/MCF-gt-PEI catalysts were evaluated in the selective hydrogenation of diphenylacetylene under identical reaction conditions. Figure 2A shows the reaction profile of diphenylacetylene conversion over the Pd−HAS ($NaBH_4$ reduction) catalyst. The yields of *trans*-stilbene and bibenzyl were very low until nearly complete conversion of diphenylacetylene was achieved in the first hydrogenation step. After the complete consumption of diphenylacetylene, *cis*-stilbene was quickly transformed into bibenzyl, while the isomerization rate to *trans*-stilbene was very low. For the Pd/SBA-gt-PEI catalyst, before the consumption of diphenylacetylene, the hydrogenation rate of diphenylacetylene and the isomerization rate of *cis*-stilbene were close to those observed over the Pd−HAS ($NaBH_4$ reduction) catalyst. However, the subsequent hydrogenation to bibenzyl was suppressed compared with the Pd−HAS ($NaBH_4$ reduction) sample (Figure 2B). Similar catalytic performance was observed with the larger-pore Pd/MCF-gt-PEI catalyst, except in this case, the rate of the second hydrogenation step to produce the alkane was even slower than that over the Pd/SBA-gt-PEI material, making this composition the most selective catalyst evaluated here (Figure 2C).

The hydrogenation rate of diphenylacetylene (R_Y), hydrogenation rate of *cis*-stilbene (R_E), and selectivity at different conversions are summarized in Table 3. All three catalysts displayed a similar diphenylacetylene hydrogenation rate, R_Y, implying that similar types and amounts of surface palladium atoms were formed in these catalysts. This is consistent with the fact that similar palladium particle sizes were observed in TEM images. A very interesting observation is that the R_E, the hydrogenation rate of the *cis*-alkene product, over the Pd−HAS ($NaBH_4$ reduction) catalyst was much higher than over the Pd/SBA-gt-PEI and Pd/MCF-gt-PEI catalysts. The MCF-supported catalyst, Pd/MCF-gt-PEI, showed the lowest *cis*-stilbene hydrogenation rate, giving a precipitous drop in the overall hydrogenation rate after complete consumption of the alkyne. According to the mechanism proposed by Molnar,[1] the high selectivity toward alkene production is due to the stronger

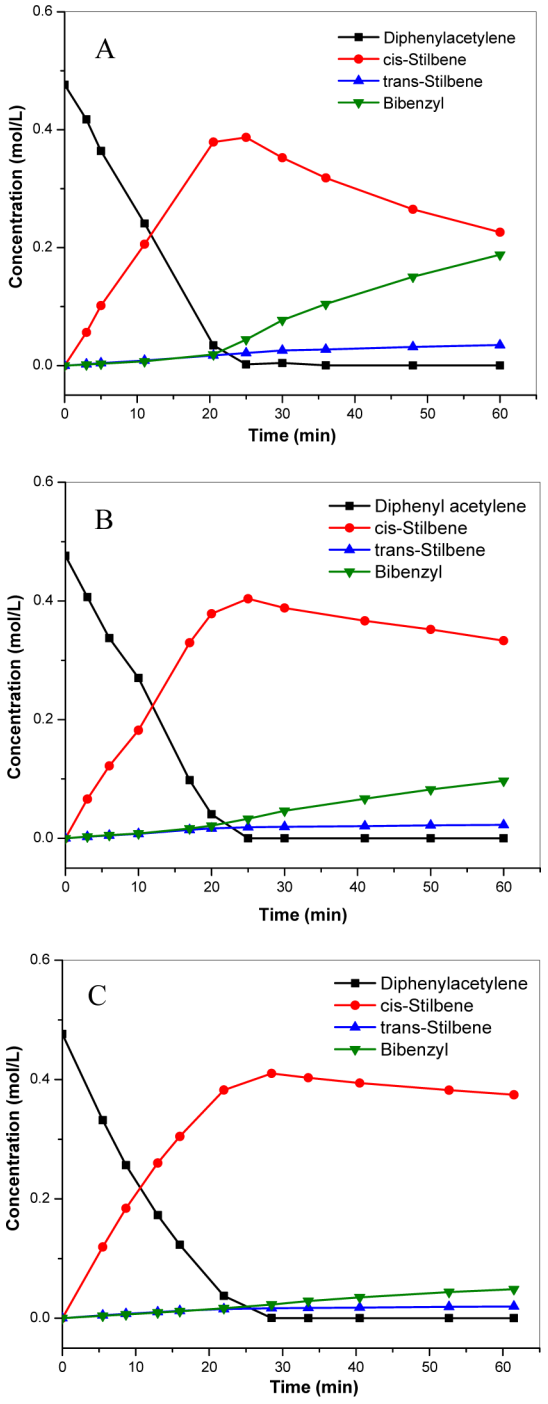

Figure 2. Reaction profiles of (A) Pd−HAS ($NaBH_4$ reduction), (B) Pd/SBA-gt-PEI, and (C) Pd/MCF-gt-PEI. Selective hydrogenation of diphenylacetylene in the mixture of MeOH and dioxane (v/v = 1:1), 0.1 mol % Pd, room temperature, 0.1 MPa H_2.

adsorption of the alkyne on the palladium surface compared with the alkene (thermodynamic control), rather than a difference in the intrinsic kinetic constants of alkyne vs olefin hydrogenation. For example, in the Lindlar catalyst, quinoline or other amines and sulfur compounds are added to the reaction mixture to compete with intermediate alkenes for the palladium active sites, thus hindering over-hydrogenation and increasing the selectivity. A recent paper by Kiwi-Minsker et al. offered a similar explanation for the selectivity of nitrogen modified Pd catalysts.[23] By modeling the experimental kinetic

dx.doi.org/10.1021/cs3007395 | ACS Catal. 2013, 3, 1700−1708

Table 3. Catalytic Performance of Aminopolymer−silica Composite Supported Pd Catalysts[a]

catalysts	R_Y[b] (h^{-1})	R_E[c] (h^{-1})	R_Y/R_E	TOF[d] (h^{-1})	conv (%)	selectivity[e]
Pd−HAS ($NaBH_4$ reduction)	3027 ± 327	794 ± 13	3.8	4800 ± 520	50	93:4:3
					93	91:4:5
Pd/SBA-gt-PEI	2598 ± 96	230 ± 16	11.2	4120 ± 150	50	92:4:4
					98	90:4:6
Pd/MCF-gt-PEI	3216 ± 12	130 ± 5	24.7	5104 ± 19	55	93:4:3
					99	92:3:5

[a]Reaction conditions: selective hydrogenation of diphenylacetylene in the mixture of MeOH and dioxane (v/v = 1:1), 0.1 mol % Pd loading, room temperature, 1 atm H_2 pressure. [b]R_Y = mol of consumed diphenylacetylene/(mol of Pd × time), R_Y calculated from the slope of the initial portion (conversion <50%) of the conversion−time plot. Each experiment was repeated twice, and the ± value represents the difference between the average and the data. [c]R_E = mol of consumed *cis*-stilbene/(mol of Pd × time). [d]TOF = mol of consumed diphenylacetylene/(mol of surface Pd atoms × time). Details of the calculations for determining the number of surface palladium atoms can be found in the Supporting Information. [e]Determined by GC−FID after calibration. Selectivity = *cis*-alkene/*trans*-alkene/alkane.

curves of the selective hydrogenation of 1-hexyne, they calculated the adsorption constants of the reactants and products in the reaction and showed the expected trend: K_1 (alkyne) > K (nitrogen compound) ≫ K_2 (alkene).

This mechanism is consistent with the experimental results in this work. In the first hydrogenation step, diphenylacetylene adsorbs on the surface of the Pd nanoparticle and is transformed into alkenes without much detrimental impact from the aminopolymer, presumably as a result of the high adsorption constant of the alkyne, leading to similar values of R_Y over the three catalysts. However, when most of the diphenylacetylene was consumed, the aminopolymer then effectively competes with alkenes for the surface palladium sites, thus blocking the active sites and reducing the subsequent hydrogenation rate. We speculate that the branched PEI used in "grafting to" catalysts could cover and passivate the palladium nanoparticles more effectively than the Pd−HAS ($NaBH_4$ reduction) catalyst, in which the polymer was of lower molecular weight, such that over-hydrogenation was further suppressed. The lower R_E of the Pd/MCF-gt-PEI catalyst than that of Pd/SBA-gt-PEI material is speculated to be because the immobilized aminopolymer may be able to more effectively swell in the larger pore space associated with the large pores in MCF, thus leading to a more effective coverage of the palladium nanoparticle surface.

3.4. Catalyst Recoverability and Recyclability. Leaching of palladium active species from the catalyst support is one of the most common reasons for deactivation of supported palladium catalysts in liquid phase reactions.[72−74] The Pd/SBA-gt-PEI was recovered after use and evaluated by elemental analysis. Table 4 shows that the palladium content of the reused

Table 4. Comparison of Compositions of the Fresh and Used Catalysts As Determined by Elemental Analysis

catalysts	Pd/SiO_2 (wt %/wt %)	Pd/N (mol/mol)	C/N (mol/mol)
Pd/SBA-gt-PEI	1.7	0.022	2.6
Pd/SBA-gt-PEI (used)	1.8	0.024	2.6

catalyst as well as that the Pd/N ratios were close to that of the fresh material, indicating no or negligible palladium leaching occurred during the reaction, suggesting the aminopolymer−silica composite was a stable support for this catalytic system. The recovered catalyst after selective hydrogenation was also characterized by HRTEM. It can clearly be observed that the size of the palladium nanoparticles was similar to that of the fresh Pd/SBA-gt-PEI, although there appears to be a slight increase in the average size to 2.2 ± 0.7 nm (Figure 1D and Supporting Information Figure S4). The recovered Pd/SBA-gt-PEI was reused for the selective hydrogenation of diphenylacetylene, resulting in a lower activity and similar selectivity compared with the fresh catalyst (Table 5), which is most likely

Table 5. Comparison of Activity and Selectivity of Fresh, Used, And Regenerated Catalysts

catalysts[a]	R_Y (h^{-1})	conv (%)	selectivity
Pd/SBA-gt-PEI	2598 ± 96	98	90:4:6
Pd/SBA-gt-PEI (used)	783 ± 105	96	91:4:5
Pd/SBA-gt-PEI (regenerated)	2661 ± 237	98	91:4:5

[a]Reaction conditions: selective hydrogenation of diphenylacetylene in the mixture of MeOH and dioxane (v/v = 1:1), 0.1 mol % Pd loading, room temperature, 1 atm H_2 pressure.

due to the increased amount of Pd(II) species (Supporting Information Table S3) formed during the purification process or in the catalytic reaction. After treatment of the used catalyst with 0.1 M $NaBH_4$, the activity of the catalysts was fully restored. The reaction profiles of Pd/SBA-gt-PEI (regenerated) displayed reaction rates similar to those of the fresh catalyst as well as the same over-hydrogenation suppression trend (Supporting Information Figure S5).

4. CONCLUSIONS

Aminopolymer−silica composite-supported Pd(0) nanoparticle catalysts with good olefin selectivity were successfully developed for the hydrogenation of alkynes in liquid media. Small palladium nanoparticles with a narrow distribution were formed on the aminopolymer−silica composite support using the $NaBH_4$ reduction method. The catalysts displayed high activity for the selective hydrogenation of diphenylacetylene while keeping very good alkene selectivity. Subsequent hydrogenation of the alkenes to alkanes was further suppressed on the Pd/SiO_2-gt-PEI catalysts compared with the Pd−HAS ($NaBH_4$ reduction), implying that better coverage of the surface of palladium nanoparticles with amino groups in the SBA-gt-PEI and MCF-gt-PEI composite catalysts prepared by the "grafting to" method using moderate molecular weight branched PEI more effectively reduced the adsorption constant of alkenes to improve the selectivity. No palladium leaching or detrimental nanoparticle agglomeration was observed in the used catalyst, and the catalytic activity could be fully recovered after regeneration of the used catalysts, indicating the excellent

dx.doi.org/10.1021/cs3007395 | ACS Catal. 2013, 3, 1700−1708

stability, recoverability, and recyclability of the catalytic system. Whereas most catalysts offer only high rates or high selectivities, these composite catalysts offer both high rates and selectivities and, thus, may be promising materials for an array of selective alkyne hydrogenations.

■ ASSOCIATED CONTENT

Supporting Information

Additional information as noted in the text. This material is available free of charge via the Internet at http://pubs.acs.org.

■ AUTHOR INFORMATION

Corresponding Author

*E-mail: cjones@chbe.gatech.edu.

Notes

The authors declare no competing financial interest.

■ ACKNOWLEDGMENTS

This work was supported by the U.S. Department of Energy, Basic Energy Sciences, for financial support through Catalysis Science Grant/Contract No. DE-FG02-03ER15459.

■ REFERENCES

(1) Molnár, Á.; Sárkány, A.; Varga, M. *J. Mol. Catal. A: Chem.* **2001**, *173*, 185−221.
(2) Crespo-Quesada, M.; Cárdenas-Lizana, F.; Dessimoz, A.-L.; Kiwi-Minsker, L. *ACS Catal.* **2012**, *2*, 1773−1786.
(3) Crespo-Quesada, M.; Yarulin, A.; Jin, M.; Xia, Y.; Kiwi-Minsker, L. *J. Am. Chem. Soc.* **2011**, *133*, 12787−12794.
(4) Semagina, N.; Renken, A.; Kiwi-Minsker, L. *J. Phys. Chem. C* **2007**, *111*, 13933−13937.
(5) Mallat, T.; Baiker, A. *Appl. Catal., A* **2000**, *200*, 3−22.
(6) Molnár, Á.; Sárkány, A.; Varga, M.; Sarkany, A. *J. Mol. Catal. A: Chem.* **2001**, *173*, 185−221.
(7) Lindlar, H. *Helv. Chim. Acta* **1952**, *35*, 446−450.
(8) Chan, C. W. A.; Tam, K. Y.; Cookson, J.; Bishop, P.; Tsang, S. C. *Catal. Sci. Technol.* **2011**, *1*, 1584−1592.
(9) Teschner, D.; Borsodi, J.; Wootsch, A.; Révay, Z.; Hävecker, M.; Knop-Gericke, A.; Jackson, S. D.; Schlögl, R. *Science* **2008**, *320*, 86−89.
(10) Tew, M. W.; Nachtegaal, M.; Janousch, M.; Huthwelker, T.; Van Bokhoven, J. A. *Phys. Chem. Chem. Phys.* **2012**, *14*, 5761−5768.
(11) Teschner, D.; Vass, E.; Havecker, M.; Zafeiratos, S.; Schnorch, P.; Sauer, H.; Knop-Gericke, A.; Schlögl, R.; Chamam, M.; Wootsch, A.; Canning, A. S.; Gamman, J. J.; Jackson, S. D.; McGregor, J.; Gladden, L. F. *J. Catal.* **2006**, *242*, 26−37.
(12) Teschner, D.; Révay, Z.; Borsodi, J.; Hävecker, M.; Knop-Gericke, A.; Schlögl, R.; Milroy, D.; Jackson, S. D.; Torres, D.; Sautet, P. *Angew. Chem., Int. Ed.* **2008**, *120*, 9414−9418.
(13) Re, Z.; Knop-Gericke, A.; Schlögl, R.; Torres, D.; Sautet, P. *J. Phys. Chem. C* **2010**, *114*, 2293−2299.
(14) García-Mota, M.; Bridier, B.; Pérez-Ramírez, J.; López, N. *J. Catal.* **2010**, *273*, 92−102.
(15) Tew, M. W.; Janousch, M.; Huthwelker, T.; Van Bokhoven, J. A. *J. Catal.* **2011**, *283*, 45−54.
(16) García-Mota, M.; Gómez-Díaz, J.; Novell-Leruth, G.; Vargas-Fuentes, C.; Bellarosa, L.; Bridier, B.; Pérez-Ramírez, J.; López, N. *Theor. Chem. Acc.* **2010**, *128*, 663−673.
(17) Bridier, B.; López, N.; Pérez-Ramírez, J. *Dalton Trans.* **2010**, *39*, 8412−8419.
(18) Mei, D.; Neurock, M.; Smith, C. M. *J. Catal.* **2009**, *268*, 181−195.
(19) López, N.; Vargas-Fuentes, C. *Chem. Commun.* **2012**, *48*, 1379−1391.
(20) Kwon, S. G.; Krylova, G.; Sumer, A.; Schwartz, M. M.; Bunel, E. E.; Marshall, C. L.; Chattopadhyay, S.; Lee, B.; Jellinek, J.; Shevchenko, E. V. *Nano Lett.* **2012**, *12*, 5382−5388.
(21) Tschan, R.; Schubert, M. M.; Baiker, A.; Bonrath, W.; Lansink-Rotgerink, H. *Catal. Lett.* **2001**, *75*, 31−36.
(22) Bridier, B.; Hevia, M.; Lopez, N.; Perez-Ramírez, J. *J. Catal.* **2011**, *278*, 167−172.
(23) Crespo-Quesada, M.; Dykeman, R. R.; Laurenczy, G.; Dyson, P. J.; Kiwi-Minsker, L. *J. Catal.* **2011**, *279*, 66−74.
(24) Lee, Y.; Motoyama, Y.; Tsuji, K.; Yoon, S.-H.; Mochida, I.; Nagashima, H. *ChemCatChem* **2012**, *4*, 778−781.
(25) Tew, M. W.; Emerich, H.; Van Bokhoven, J. A. *J. Phys. Chem. C* **2011**, *115*, 8457−8465.
(26) Osswald, J.; Kovnir, K.; Armbruester, M.; Giedigkeit, R.; Jentoft, R. E.; Wild, U.; Grin, Y.; Schlögl, R. *J. Catal.* **2008**, *258*, 219−227.
(27) Guczi, L.; Schay, Z.; Stefler, G.; Liotta, L. F.; Venezia, A. M. *J. Catal.* **1999**, *182*, 456−462.
(28) Vicente, A.; Lafaye, G.; Especel, C.; Marécot, P.; Williams, C. T. *J. Catal.* **2011**, *283*, 133−142.
(29) Anderson, J. A.; Mellor, J.; Wells, R. P. K. *J. Catal.* **2009**, *261*, 208−216.
(30) Mori, S.; Ohkubo, T.; Ikawa, T.; Kume, A.; Maegawa, T.; Monguchi, Y.; Sajiki, H. *J. Mol. Catal. A: Chem.* **2009**, *307*, 77−87.
(31) Drelinkiewicz, A.; Stanuch, W.; Knapik, A.; Ghanem, A.; Kosydar, R.; Bukowska, A.; Bukowski, W. *J. Mol. Catal. A: Chem.* **2009**, *300*, 8−18.
(32) Sajiki, H.; Mori, S.; Ohkubo, T.; Ikawa, T.; Kume, A.; Maegawa, T.; Monguchi, Y. *Chem.—Eur. J.* **2008**, *14*, 5109−5111.
(33) Evangelisti, C.; Panziera, N.; D'Alessio, A.; Bertinetti, L.; Botavina, M.; Vitulli, G. *J. Catal.* **2010**, *272*, 246−252.
(34) Drelinkiewicz, A.; Knapik, A.; Stanuch, W.; Sobczak, J.; Bukowska, A.; Bukowski, W. *React. Funct. Polym.* **2008**, *68*, 1652−1664.
(35) Liu, W.; Otero Arean, C.; Bordiga, S.; Groppo, E.; Zecchina, A. *ChemCatChem* **2011**, *3*, 222−226.
(36) Na-Chiangmai, C.; Tiengchad, N.; Kittisakmontree, P.; Mekasuwandumrong, O.; Powell, J.; Panpranot, J. *Catal. Lett.* **2011**, *141*, 1149−1155.
(37) Papp, A.; Molnár, Á.; Mastalir, Á. *Appl. Catal., A* **2005**, *289*, 256−266.
(38) Marín-Astorga, N.; Pecchi, G.; Pinnavaia, T. J.; Alvez-Manoli, G.; Reyes, P. *J. Mol. Catal. A: Chem.* **2006**, *247*, 145−152.
(39) Mastalir, Á.; Király, Z.; Szöllösi, G.; Bartók, M. *J. Catal.* **2000**, *194*, 146−152.
(40) Mastalir, Á.; Szabó, T.; Király, Z.; Dékány, I. *Catal. Commun.* **2012**, *17*, 104−107.
(41) Lee, K. H.; Lee, B.; Lee, K. R.; Yi, M. H.; Hur, N. H. *Chem. Commun.* **2012**, *48*, 4414.
(42) Mastalir, Á.; Király, Z. *J. Catal.* **2003**, *220*, 372−381.
(43) Jackson, S. D.; Shaw, L. A. *Appl. Catal., A* **1996**, *134*, 91−99.
(44) White, R. J.; Luque, R.; Budarin, V. L.; Clark, J. H.; Macquarrie, D. J. *Chem. Soc. Rev.* **2009**, *38*, 481−494.
(45) Kluwer, A. M.; Koblenz, T. S.; Jonischkeit, T.; Woelk, K.; Elsevier, C. J. *J. Am. Chem. Soc.* **2005**, *127*, 15470−15480.
(46) Van Laren, M. W.; Elsevier, C. J. *Angew. Chem., Int. Ed.* **1999**, *38*, 3715−3717.
(47) Van Laren, M. W.; Duin, M. A.; Klerk, C.; Naglia, M.; Rogolino, D.; Pelagatti, P.; Bacchi, A.; Pelizzi, C.; Elsevier, C. J. *Organometallics* **2002**, *21*, 1546−1553.
(48) Pelagatti, P.; Venturini, A.; Leporati, A. *J. Chem. Soc., Dalton Trans.* **1998**, 2715−2721.
(49) Costa, M.; Pelagatti, P.; Pelizzi, C.; Rogolino, D. *J. Mol. Catal. A: Chem.* **2002**, *178*, 21−26.
(50) Liprandi, D. A.; Cagnola, E.; Quiroga, M. *Catal. Lett.* **2009**, *128*, 423−433.
(51) Evrard, D.; Groison, K.; Mugnier, Y.; Harvey, P. D. *Inorg. Chem.* **2004**, *43*, 790−796.
(52) Mizugaki, T.; Ooe, M.; Ebitani, K.; Kaneda, K. *J. Mol. Catal. A: Chem.* **1999**, *145*, 329−333.
(53) Crooks, R. M.; Zhao, M.; Sun, L.; Chechik, V.; Yeung, L. K. *Acc. Chem. Res.* **2001**, *34*, 181.

(54) Semagina, N.; Joannet, E.; Parra, S.; Sulman, E.; Penken, A.; Kiwi-Minskerr, L. *Appl. Catal., A* **2005**, *280*, 141.
(55) Bönnemann, H.; Brijoux, W.; Siepen, K.; Hormes, J.; Franke, R.; Pollman, J.; Rothe, J. *Appl. Organomet. Chem.* **1997**, *11*, 783.
(56) Li, D.; Wang, C.; Tripkovic, D.; Sun, S.; Markovic, N. M.; Stamenkovic, V. R. *ACS Catal.* **2012**, *2*, 1358.
(57) Corain, B. *J. Mol. Catal. A: Chem.* **2001**, *173*, 99.
(58) Jiang, Y.; Gao, Q. *J. Am. Chem. Soc.* **2006**, *128*, 716.
(59) Biradar, A. V; Biradar, A. A.; Asefa, T. *Langmuir* **2011**, *27*, 14408.
(60) Lukens, W. W.; Schmidt-Winkel, P.; Zhao, D.; Feng, J.; Stucky, G. D. *Langmuir* **1999**, 5403−5409.
(61) Zhao, D.; Huo, Q.; Feng, J.; Chmelka, B. F.; Stucky, G. D. *J. Am. Chem. Soc.* **1998**, *120*, 6024−6036.
(62) Zhao, D.; Feng, J.; Huo, Q.; Melosh, N.; Fredrickson, G. H.; Chmelka, B. F.; Stucky, G. D. *Science* **1998**, *279*, 548.
(63) Han, Y.; Lee, S. S.; Ying, J. Y. *Chem. Mater.* **2007**, *19*, 2292.
(64) Kim, H.; Moon, J.; Park, J. *J. Colloid Interface Sci.* **2000**, *227*, 247.
(65) Hicks, J. C.; Drese, J. H.; Fauth, D. J.; Gray, M. L.; Qi, G.; Jones, C. W. *J. Am. Chem. Soc.* **2008**, *130*, 2902.
(66) Kim, S.; Ida, J.; Guliants, V. V; Lin, J. Y. S. *J. Phys. Chem. B* **2005**, *109*, 6287−6293.
(67) Krämer, M.; Stumbé, J.; Grimm, G.; Kaufmann, B.; Krüger, U.; Weber, M.; Haag, R. *ChemBioChem* **2004**, *5*, 1081.
(68) Amali, A. J.; Rana, R. K. *Green Chem.* **2009**, *11*, 1781.
(69) Moreno, M.; Ibañez, F. J.; Jasinski, J. B.; Zamborini, F. P. *J. Am. Chem. Soc.* **2011**, *133*, 4389.
(70) Drese, J. H.; Choi, S.; Lively, R. P.; Koros, W. J.; Fauth, D. J.; Gray, M. L.; Jones, C. W. *Adv. Funct. Mater.* **2009**, *19*, 3821−3832.
(71) Drese, J. H.; Choi, S.; Didas, S. A.; Bollini, P.; Gray, M. L.; Jones, C. W. *Microporous Mesoporous Mater.* **2012**, *151*, 231.
(72) Köhler, K.; Heidenreich, R. G.; Krauter, J. G. E.; Pietsch, J. *Chem.—Eur. J.* **2002**, *8*, 622.
(73) Phan, N. T. S.; Van Der Sluys, M.; Jones, C. W. *Adv. Synth. Catal.* **2006**, *348*, 609−679.
(74) Astruc, D. *Inorg. Chem.* **2007**, *46*, 1884.